

A STUDY OF ACETIC ACID ROLE IN CO₂ CORROSION

By

Syed Sadiq Bin Syed Sheikh

10017

Dissertation submitted in partial fulfilment of
the requirements for the
Bachelor of Engineering (Hons)
(Mechanical Engineering)

MAY 2011

Universiti Teknologi PETRONAS

Bandar Seri Iskandar

31750 Tronoh

Perak Darul Ridzuan

CERTIFICATION OF APPROVAL

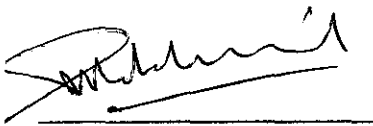
A STUDY OF ACETIC ACID ROLE IN CO₂ CORROSION

by

Syed Sadiq Bin Syed Sheikh

A project dissertation submitted to the
Mechanical Engineering Programme
Universiti Teknologi PETRONAS
in partial fulfilment of the requirement for the
BACHELOR OF ENGINEERING (Hons)
(MECHANICAL ENGINEERING)

Approved by,



(AP Ir. Dr. Mokhtar Che Ismail)

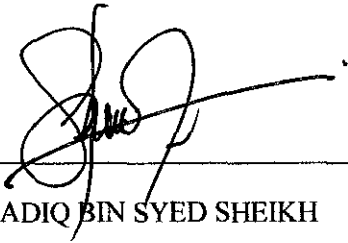
UNIVERSITI TEKNOLOGI PETRONAS

TRONOH, PERAK

May 2011

CERTIFICATION OF ORIGINALITY

This is to certify that I am responsible for the work submitted in this project, that the original work is my own except as specified in the references and acknowledgements, and that the original work contained herein have not been undertaken or done by unspecified sources or persons.

A handwritten signature in black ink, consisting of stylized loops and a long horizontal stroke extending to the right, positioned above a horizontal line.

SYED SADIQ BIN SYED SHEIKH

LIST OF FIGURES

| | | |
|-----------|---|----|
| Figure 1 | Non-linear I-V curve | 9 |
| Figure 2 | Low amplitude sine wave | 10 |
| Figure 3 | A typical Nyquist plot | 11 |
| Figure 4 | A typical Bode plot | 12 |
| Figure 5 | Schematic diagram for the set-up | 14 |
| Figure 6 | Experiment flowchart | 14 |
| Figure 7 | Images of the test set up | 18 |
| Figure 8 | Corrosion rate at 0 ppm of HAc | 20 |
| Figure 9 | Corrosion rate at 1000 ppm of HAc | 21 |
| Figure 10 | Corrosion rate at 2000 ppm of HAc | 21 |
| Figure 11 | Corrosion Rate at 4000 ppm of HAc | 22 |
| Figure 12 | Graph of corrosion rate vs acetic acid concentrations | 22 |
| Figure 13 | Corrosion Rate at 4 various concentrations of HAc | 23 |
| Figure 14 | Nyquist plot at 0 ppm of HAc | 24 |
| Figure 15 | Nyquist plot at 1000 ppm of HAc | 25 |
| Figure 16 | Nyquist plot at 2000 ppm of HAc | 25 |
| Figure 17 | Nyquist plot at 4000 ppm of HAc | 26 |
| Figure 18 | Nyquist plot of the effect of HAc at four different concentrations | 26 |
| Figure 19 | SEM micrographs for X52 carbon steel achieved after 2 h of exposure in CO ₂ -saturated 3wt% NaCl solution at the temperature of 60°C under 500X magnification in the presence of (a) 0, (b) 1000, (c) 2000, and (d) 4000 ppm of acetic acid | 29 |
| Figure 20 | SEM micrographs for X52 carbon steel achieved after 2 h of exposure in CO ₂ -saturated 3wt% NaCl solution at the temperature of 60°C under 1000X magnification in the presence of (a) 0, (b) 1000, (c) 2000, and (d) 4000 ppm of acetic acid | 29 |
| Figure 21 | SEM micrographs for X52 carbon steel achieved after 2 h of exposure in CO ₂ -saturated 3wt% NaCl solution at the temperature of 60°C under 5000X magnification in the presence of (a) 0, (b) 1000, (c) 2000, and (d) 4000 ppm of acetic acid | 30 |

| | | |
|-----------|---|----|
| Figure 22 | XRD analysis of the layer formed on the X52 carbon steel at pH 5.5 and T=60°C in the absence of acetic acid and in the presence of 4000 ppm of acetic acid after 2h | 32 |
| Figure 23 | XRD analysis of the layer formed on the X52 carbon steel at pH 5.5 and T=60°C in the absence of acetic acid after 2h. | 32 |
| Figure 24 | XRD analysis of the layer formed on the X52 carbon steel at pH 5.5 and T=60°C in the presence of 4000 ppm of undissociated acetic acid after 2h. | 33 |

LIST OF TABLES

| | | |
|---------|---|----|
| Table 1 | Test matrix for the experiment | 13 |
| Table 2 | Acetic acid concentration at pH 5.5 and 60°C | 13 |
| Table 3 | Elemental composition of X52 carbon steel based on wt % | 16 |

ACKNOWLEDGEMENTS

First of all, I would like to express my deepest gratitude to God The Mightiest for His blessing & guidance for me in completing Final Year Project.

My honest and highest appreciation goes to my supervisor; AP Ir. Dr. Mokhtar Che Ismail for his effort in supervising & guiding me towards completing my Final Year Project as partial fulfillment of the requirement for the Bachelor of Engineering (Hons) of Mechanical Engineering.

Many figures had provided immeasurable amount of guidance, ideas, assistance, support and advice. Without help from these people, this Final Year Project may not be that meaningful and successful. Greatest appreciation is expressed to Mr. Martin Choirul Fatah for his invaluable teachings, advices, and critiques in ensuring my project ran smoothly and completed successfully.

Furthermore I would like to give my special word of appreciation to all Mechanical Engineering lecturers and technicians, especially Mr. Faisal and Mr. Irwan who has assisted me in analyzing the results and completing my project.

Thousands of appreciations are also extended to my family and friends for their full support, kindness, assistance, guidance and criticisms during the whole period of finishing my project.

Last but not least, thank you very much to anyone who has assisted me directly or indirectly in making my Final Year Project a success.

ABSTRACT

The presence of organic acids typically acetic acid (HAc) in reservoir is known to influence CO₂ corrosion. However, the mechanism of the higher concentration of HAc on CO₂ corrosion is still unclear. The role of higher concentration of HAc in CO₂ corrosion needs to be determined for accurate corrosivity prediction. The aim of the project is to understand the role of different concentrations of HAc on CO₂ corrosion. The role of HAc in CO₂ corrosion is investigated by using electrochemical impedance spectroscopy (EIS), linear polarization resistance (LPR), scanning electron microscopy (SEM), and x-ray diffraction (XRD) techniques. All experiments were conducted in a 3% NaCl solution of pH 5.5 and temperature 60°C. In the absence of HAc, CO₂ corrosion produced iron carbonate film which comes from the reaction of iron ions and carbonate ions. At 1000 ppm and 2000 ppm HAc, a layer of iron acetate (FeAc) seems to form and solubilize continuously since the rate of formation of FeAc is much higher than that of FeCO₃. By adding 4000 ppm of HAc, the FeAc layer seems to grow due to the excessive amount of HAc and finally forming a layer on the steel surface, thus reducing the corrosion rate. This behavior is shown by the EIS curves for each concentrations of acetic acid. The formation of FeAc layer can be seen in the SEM micrographs and the presence of FeAc is confirmed by using the XRD technique.

TABLE OF CONTENT

| | |
|---|-------------|
| CERTIFICATION OF APPROVAL | ii |
| CERTIFICATION OF ORIGINALITY | iii |
| LIST OF FIGURES | iv |
| LIST OF TABLES | v |
| ACKNOWLEDGEMENT | vi |
| ABSTRACT | vii |
| TABLE OF CONTENT | viii |
| CHAPTER 1: INTRODUCTION | 1 |
| 1.1. Project Background | 1 |
| 1.2. Problem Statement | 2 |
| 1.3. Objective | 2 |
| CHAPTER 2: LITERATURE REVIEW | 3 |
| 2.1. CO ₂ Corrosion | 3 |
| 2.2. Acetic Acid Corrosion | 4 |
| 2.3. Iron Carbonate (FeCO ₃) Film Formation | 7 |
| 2.4. Electrochemical Impedance Spectroscopy (EIS) | 9 |
| CHAPTER 3: METHODOLOGY | 13 |
| 3.1. Test Matrix | 13 |
| 3.2. Experimental Setup | 14 |
| 3.3. Experiment Procedure | 14 |
| 3.4. Electrochemical Test Methods | 16 |
| 3.5. Gantt Chart | 19 |
| CHAPTER 4: RESULTS & DISCUSSION | 20 |
| 4.1 Data Gathering & Analysis | 20 |

CHAPTER 5: CONCLUSION & RECOMMENDATIONS 34

REFERENCES 35

1. INTRODUCTION

1.1 Project Background

Carbon dioxide (CO₂) corrosion is one the most studied form of corrosion in oil and gas industry. This is generally due to the fact that the crude oil and natural gas from the oil reservoir/gas well usually contains some level of CO₂ and hydrogen sulfide (H₂S). The major concern with CO₂ corrosion in oil and gas industry is that CO₂ corrosion can cause failure on the equipment especially the main downhole tubing and transmission pipelines and thus can disrupt the oil/gas production. The presence of carbon dioxide (CO₂), hydrogen sulfide (H₂S) and free water can cause severe corrosion problems in oil and gas pipelines. Internal corrosion in wells and pipelines is influenced by temperature, CO₂ and H₂S content, water chemistry, flow velocity, oil or water wetting and composition and surface condition of the steel. A small change in one of these parameters can change the corrosion rate drastically due to changes in the properties of the thin layer of corrosion products that accumulates on the steel surface.

CO₂ corrosion in the presence of acetic acid (HAc) is recognized as a major course of premature failure of mild steel pipelines in the oil and gas industry. CO₂ is present as a dissolved gas in the water /brine that accompanies oil production at high pressures common in underground oil and gas reservoirs. In the dissolved state it forms carbonic acid. Premature failure is caused by the presence of a complex variety of flow regimes, multiphase flow conditions and the presence of HAc. The material of construction for pipelines in the oil and gas industry is carbon steel for majority of facilities in production installations, because of its economical price, strength, and availability. However, carbon steel has a tendency to corrode in the presence of CO₂ and HAc. It is therefore important to investigate the conditions in which HAc causes corrosion damage.

The choice of the materials may also contribute to the effect of corrosion rate of a material. It is believed that certain materials may increase the corrosion rate, some may reduce it, and some may make the corrosion rate become constant when certain temperatures are reached. Predictions are being made on the corrosion rate due to the selection of materials by considering the mechanical properties of the material, its corrosion resistance, as well as its thermal conductivity. However, thorough investigation and studies need to be made in order to get more accurate data on the relationship between the corrosion rate and the material selection.

In CO₂ corrosion, iron carbonate (FeCO₃) film is the chief corrosion product formed and is formed through the reaction between carbonic acid that are released through corrosion of the pipeline. FeCO₃ forms on the wall of the pipe if the product of ferrous ion concentration (Fe²⁺) and carbonate ion concentration (CO₃²⁻) exceeds the solubility product limit. The film is known to be protective and the corrosion rate drops once the film starts growing. Although studies has been made on iron carbonate film formation mechanisms and kinetics, it is not known how protective the film will be in the presence of HAc. Thus, it becomes imperative to understand how FeCO₃ precipitation is affected in the presence of HAc, as also by the temperature and ionic strength of the solution.

1.2 Problem Statement

CO₂ corrosion is often influenced by the presence of organic acid, particularly acetic acid. CO₂ corrosion in the presence of acetic acid can lead to premature failure in oil and gas pipelines which can results in millions of dollars in property damage besides lost of production and bodily injury. Therefore, there is a need to understand the role of acetic acid in CO₂ corrosion so that the representative corrosion protection can be made in order to reduce the corrosion rate and to prevent corrosion.

1.3 Objective

The objective of this project is to study and understand the role and effect of various concentrations of acetic acid on CO₂ corrosion.

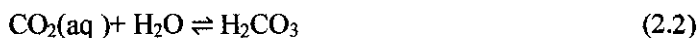
2.LITERATURE REVIEW

2.1 CO₂ Corrosion

CO₂ corrosion of steel has been the subject of a wide area of research through the decades with reference to issues of corrosion and pipeline failure in the oil and gas production and transportation industry. Although the factors which influence the rate and type of corrosion have been identified, the interactions between them at various conditions are still the subject of research today[1]. Dry CO₂ gas by itself is not corrosive at the temperatures encountered within oil and gas production. It needs to be dissolved in an aqueous phase to promote an electrochemical reaction between steel and the contacting aqueous phase[5]. CO₂ is soluble in water and brines. However, it should be noted that it has a similar solubility in both the gaseous and liquid hydrocarbon phases. Thus, for a mixed-phase system, the presence of the hydrocarbon phase may provide a ready reservoir of CO₂ to partition into the aqueous phase[5].

Corrosion of carbon steel in CO₂-containing environments is a very complex phenomenon and still requires further elucidation. Various mechanisms have been proposed for the process. However, these either apply to very specific conditions or have not received widespread recognition and acceptance[5]. Omkar (2004)[1] stated that one of the earliest efforts to explain the mechanism of CO₂ corrosion was explained by de Waard and Milliams (1975). More recent studies (1995, 2001,2003) have proposed models to predict CO₂ corrosion of mild steels based on their independent body of work. The following is a summary of reactions which define CO₂ corrosion.

CO₂ dissolves in water to form carbonic acid through the hydration of water.



Carbonic acid dissociates to form bicarbonate which also dissociates to give carbonate and hydrogen ions.



de Waard and Milliams explained that the rate determining step for carbonic acid dissociation is the direct reduction of carbonic acid (H_2CO_3) and the corrosion rate is governed by the amount of undissociated acid in solution[1].



The corresponding iron dissolution reaction is



The insoluble corrosion product of reactions (2.3), (2.4), and (2.7) is iron carbonate which forms by the reaction



2.2 Acetic Acid Corrosion

The influence of HAc on the rate of corrosion of mild steel in oilfield brines containing CO_2 is well documented in literature and has been the subject of numerous studies since the 1980's[1]. Its presence was categorized together with organic acids or based on the measurement of a mean molecular weight of organic acids, that of propionic acid. Addition of acetic acid to the test environment reduces the protectiveness of the films and increases the sensitivity to mesa attack. This attributes to a lower Fe^{2+} supersaturation in the corrosion film and at the steel surface. Significant reduction in film stability was observed when the concentration of undissociated HAc in the solution was increased from 0.05 mmol to 0.2 mmol, but the results are too few to give more accurate threshold values[5]. In the case of carbon steel in brine, the dominating factor influencing the corrosion rate is the presence of acetate (Ac^-) and dissolved CO_2 gas resulting in the formation of acetic acid[1]. In this situation, genuine acetic acid corrosion occurs, controlled by the solubility equilibrium with a gas phase containing HAc vapor, as in the case of CO_2 corrosion.

Omkar (2004)[1] in his studies also stated that as early as 1983, Crolet and Bonis reported that the presence of acetic acid in the brine could increase the corrosion rate of carbon steel significantly. They also make the point that CO_2 induced acidification can cause partial reassociation of anions, such as acetates and propionates, to form organic acids. Such

weak acids then will increase the oxidizing power of H^+ by raising the limiting diffusion current for cathodic reduction[5]. The presence of such acids also will tend to solubilize the dissolving iron ions suppress $FeCO_3$, or oxide film formation, which can otherwise passivate the steel surface[5]. Omkar (2004)[1] said that Hedges and McVeigh (1999) later confirmed this but the interconversion of HAc and Ac^- ions as given by Equation (2.9) was not accounted for. In the presence of Ac^- ions, the corrosion rate can increase even if the pH increases leading to errors in prediction models for corrosion rates. The presence of both HCO_3^- and Ac^- cause erroneous titration results leading to an overestimation of pH.

The presence of acetate (Ac^-) is the result of which comes from the dissociation of HAc



leads to an overestimation of pH when the HCO_3^- analysis is carried out leading to significant under prediction of corrosion rates. The equilibrium constant for equation (2.9) is K_{HAc} and expressed as

$$K_{HAc} = \frac{[H^+][Ac^-]}{[HAc]} \quad (2.10)$$

K_{HAc} is dependent on temperature (T_c , Celcius) and was first expressed by Kharaka (1989)[1]

$$K_{HAc} = 10^{-(6.66104 - 0.0134916 * (273 + T_c) + 2.37856 * 10^{-5} * (273 + T_c)^2)} \quad (2.11)$$

In equation 2.10 the total amount of HAc, $[HAc]$ and the temperature are known. So, K_{HAc} is also known. Thus the concentration of H^+ ions, $[H^+]$ or the pH value determines how much of the acetic acid will dissociate. Thus different pH values represent different amounts of undissociated (free) HAc which is the main cause of concern as it was found to increase the corrosion rate. HAc acts as a reservoir of H^+ ions, which readily accept electrons produced by the iron dissolution reaction. George (2003)[14] suggested that HAc does not affect the charge transfer mechanism of the cathodic reaction but only affects the limiting currents. The corrosion rate of X-65 carbon steel in the presence of HAc is under charge transfer control and both the anodic and cathodic reactions remained the same. Acetic acid was found to increase X-65 carbon steel corrosion rates greatly at pH 4 as found from a series of experiment conducted.

Omkar (2004)[1] stated that Sidorin (2003) did voltammetry experiments on steel rotating disc electrode (RDE) and found that solutions containing Ca^{2+} and Fe^{2+} ions do not change the equilibrium concentration of HAc significantly although they increase the ionic strength of the solution.

Crolet et al. (1999)[12] showed that for uniform corrosion beneath a protective layer the free HAc is exhausted and in such a situation the acetic buffer was decisive in determining the protectiveness of corrosion products. He also reported an inhibition of the anodic dissolution reaction of iron in presence of Ac^- ions.

Garsany et al. (2002,2003)[15] in their work used cyclic voltammetry to study the effect of Ac^- ions on the rates of corrosion using a rotating disc electrode (RDE) in the absence of film formation. They emphasized that the electrochemistry of acetic acid at steel cannot be distinguishable from that of free proton (because of its rapid dissociation) and predicted that the increased rate of corrosion is proportional to the concentration of undissociated acetic acid in the brine.

Joosten et al. (2002)[13] examined acetic acid, synthetic seawater and an oil phase in glass cells and found that HAc increased the corrosion rate by decreasing the pH. He also found evidence of localized 13% Cr steel at 95°C and 600 ppm HAc.

George (2003)[14] investigated the effects of HAc on the cathodic and anodic reactions of CO_2 corrosion using Linear Polarization Resistance (LPR), Electrochemical Impedance Spectroscopy (EIS), and potentiodynamics sweeps. He concluded that HAc did not affect the charge transfer mechanism of the cathodic reaction but did affect the limiting currents. At room temperature (22°C) the HAc acts as a source of hydrogen ions and HAc needs an "activation time" for its effect to be measured.

Mehdi (2010)[6] mentioned that, based on the study from Nafday and Nestic, HAc cannot cause any localized corrosion, has no effect on the thickness of corrosion product iron carbonate (FeCO_3) layer but affects layer morphology. However, Okafor and Nestic reported that acetic acid can cause localized corrosion by removing iron carbonate layer. He also stated that George and Nestic reported the presence of HAc strongly affects the cathodic limiting current. The anodic reaction (iron dissolution) was unaffected or mildly retarded with increasing HAc concentration at room temperature.

Liu et al. (2008)[16] investigated the effect of HAc using electrochemical impedance spectroscopy (EIS). They found that the surface chemical reactions of cathodic reduction were enhanced in the presence of HAc. They also found that HAc can remove FeCO₃ layer. Zhang and Cheng (2009)[8] reported similar results. In addition, they observed an increase in the current density of anodic reactions and they saw localized corrosion on the surface of steel.

Thus experiments of long duration (3 days) were conducted at film forming conditions of high temperature (80°C) and high pH to see the the effect of HAc on the film and the corrosion rate.

2.3 Iron Carbonate (FeCO₃) Film Formation

Iron carbonate (FeCO₃) film formation is the main corrosion product in the CO₂ corrosion proces. Film formation is strongly dependent on the thermodynamics and kinetics of FeCO₃ precipitation. Supersaturation plays the most important role in FeCO₃ film growth and its morphology. A high supersaturation of FeCO₃ is necessary to form a protective film, particularly at low temperatures[5]. In principle, the precipitation process comprises two steps, nucleation and particle growth. The morphology of the film therefore depends on the dominating step[5]. The reaction for formation of solid iron carbonate is given by:



FeCO₃ forms on the wall of the pipe if the product of ferrous ion concentration (Fe²⁺) and carbonate ion concentration (CO₃²⁻) exceeds the solubility product limit[1]. A measure of when the film is likely to precipitate is supersaturation value (SS) defined as

$$SS = \frac{[\text{Fe}^{2+}][\text{CO}_3^{2-}]}{[K_{sp\text{FeCO}_3}]} \quad (2.13)$$

The film will precipitate when the SS value exceeds unity. However, the rate of precipitation of iron carbonate can be so slow that often the precipitation kinetics becomes more important than the thermodynamics of the process. The equilibrium constant for iron carbonate film K_{spFeCO₃} is dependent on temperature (Tc, Celcius) and ionic strength (I) and expressed as

$$K_{sp\text{FeCO}_3} = 10^{(-10.13 - 0.0182 * T_c)} / (0.0115 * I^{0.6063}) \quad (2.14)$$

$$I = 0.5 * \sum nZ^2 \quad (2.15)$$

where l represents the number of ions, Z is charge of each ion and n is the molar concentration of each ion[1].

FeCO_3 reduces the corrosion rate by reducing and virtually sealing film porosity[5]. With altering neither the local phase compositions nor the concentration gradient, this restricts the diffusion fluxes of the species involved in the electrochemical reactions. Moreover, even prior to sealing cementite its precipitation can lead to coverage and, therefore, can limit its electrochemical activity. It is also believed that increasing the temperature would improve the protectiveness of the FeCO_3 scale as well as its adhesion and hardness and that the higher the temperature, the more improved the protectiveness[5]. However, there is a little agreement on a practical “threshold” temperature. Some have reported that the maximum corrosion rate observed for carbon steel in sweet environments was from 60°C to 70°C and then it started to decline due to growth of protective FeCO_3 films[5]. In another studies[5], it has been suggested that the lowest temperature necessary to obtain FeCO_3 films that would reduce the corrosion rate significantly was 50°C and the protectiveness was increased also by increasing the pH.

From a study, Omkar (2004)[1] mentioned that Johnson and Tomson (1991) used a “temperature ramped” approach to calculate the activation energy of FeCO_3 precipitation and found that precipitation was controlled by the surface reaction rate. The most important factors which affect the precipitation of iron carbonate film are supersaturation and temperature. The film is known to be protective and corrosion rate drops once the film starts growing. When FeCO_3 protective film forms, its growth is very temperature sensitive. Its composition, structure and thickness and physical properties are determined by the film precipitation mechanisms. A frequently used expression for the rate of precipitation of iron carbonate ($R_{\text{FeCO}_3(s)}$) is given by Van Hunnik et al. (1996) as stated by Omkar (2004)[1]

$$R_{\text{FeCO}_3(s)} = \frac{A}{V} \cdot f(T) \cdot K_{sp} \cdot f(SS) \quad (2.16)$$

where A is the surface area of the electrode and V is the solution volume.

Since CO_3^{2-} ion concentration is dependent on the pH, we can write

$$SS = f(\text{Fe}^{2+}, \text{pH}) \quad (2.17)$$

When iron carbonate precipitates at the steel surface, it decreases the corrosion rate by

- Presenting a diffusion barrier for the species involved in the corrosion process
- Blocking a portion of the steel and preventing electrochemical reactions from occurring.

Studies by Ikeda et al. (1984), as mentioned by Omkar (2004)[1] indicate three types of films: at low temperatures ($<60^{\circ}\text{C}$) the film is not adherent and is easily destroyed, at 60°C - 150°C a loosely adherent FeCO_3 precipitate causes deep pitting and very high corrosion rates, at temperatures $>150^{\circ}\text{C}$ an adherent scale forms limiting corrosion. Omkar (2004)[1] concluded that the film can be formed at room temperature by increasing system pH as indicated by Videm and Dugstad (1989). Dugstad (1992) showed that films were formed at 80°C after only 20-24 hours.

2.4 Electrochemical Impedance Spectroscopy (EIS)

EIS has been successfully applied to the study of corrosion systems for thirty years and been proven to be a powerful and accurate method for measuring corrosion rates. But in order to access the charge transfer resistance or polarization resistance that is proportional to the corrosion rate at the monitored interface, EIS results have to be interpreted with the help of a model of the interface.

An important advantage of EIS over other laboratory techniques is the possibility of using very small amplitude signals without significantly disturbing the properties being measured. The fundamental approach of all impedance methods is to apply a small amplitude sinusoidal excitation signal to the system under investigation and measure the response (current or voltage or another signal of interest). In figure 1 and Figure 2 below, a non-linear I-V curve and a low amplitude sine wave for a theoretical electrochemical system is shown.

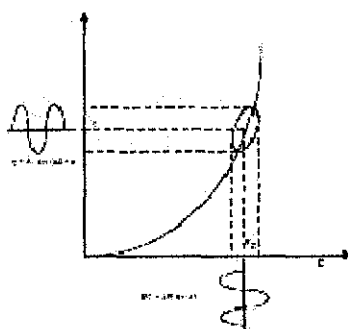


Figure 1: Non-linear I-V curve

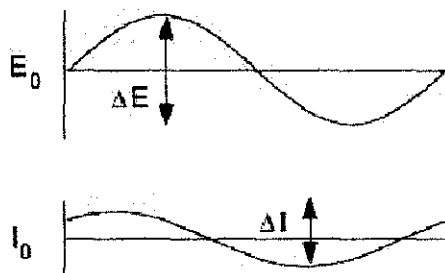


Figure 2: Low amplitude sine wave

A low amplitude sine wave $\Delta E \sin(\omega t)$, of a particular frequency, is superimposed on the dc polarization voltage E_0 . This results in a current response of a sine wave $\Delta I \sin(\omega t + \phi)$ superimposed on the dc current I_0 . The current response is shifted with respect to the applied potential. The Taylor series expansion for the current is given by

$$\Delta I = \left(\frac{dI}{dE}\right)_{E_0, I_0} \Delta E + \frac{1}{2} \left(\frac{d^2 I}{dE^2}\right)_{E_0, I_0} \Delta E + \dots \quad (2.18)$$

If the magnitude of the perturbing signal ΔE is small, then the higher order terms

$$\frac{1}{2} \left(\frac{d^2 I}{dE^2}\right)_{E_0, I_0} \Delta E + \dots \quad (2.19)$$

in the first equation can be assumed to be negligible. The impedance of the system can then be calculated using Ohm's law as,

$$Z(\omega) = \frac{\Delta E(\omega)}{\Delta I(\omega)} \quad (2.20)$$

This ratio is called impedance, $Z(\omega)$, of the system and is a complex quantity with a magnitude and a phase shift which depends on the frequency of the signal. Therefore by varying the frequency of the applied signal one can get the impedance of the system as a function of frequency. Typically in electrochemistry, a frequency range of 100 kHz – 0.1 Hz is used. The impedance, $Z(\omega)$, as mentioned above is a complex quantity and can be represented in Cartesian as well as polar co-ordinates.

In polar co-ordinates the impedance of the data is represented by,

$$Z(\omega) = |Z(\omega)|e^{j\phi(\omega)} \quad (2.21)$$

where $|Z|$ is magnitude of the impedance and ϕ is the phase shift.

$$Z(\omega) = Z_r(\omega) + jZ_j(\omega) \quad (2.22)$$

where Z_r is the real part of the impedance and Z_j is the imaginary part and $j = \sqrt{-1}$

The plot of the real part of impedance against the imaginary part gives a Nyquist Plot, as shown in Figure 3. The advantage of Nyquist representation is that it gives a quick overview of the data and one can make some qualitative interpretations. While plotting data in the Nyquist format the real axis must be equal to the imaginary axis so as not to distort the shape of the curve. The shape of the curve is important in making qualitative interpretations of the data. The disadvantage of the Nyquist representation is that one loses the frequency dimension of the data. One way of overcoming this problem is by labelling the frequencies on the curve.

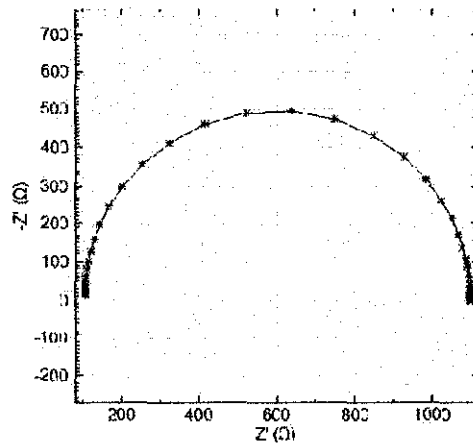


Figure 3: A typical Nyquist plot

The absolute value of impedance and the phases shifts are plotted as a function of frequency in two different plots giving a Bode Plot, as shown in figure 4. This is the more complete way of presenting the data. The relationship between the two ways of representing the data is as follows:

$$|Z|^2 = (Re Z)^2 + (Im Z)^2 \quad (2.23)$$

$$\phi = \tan^{-1} \frac{Im Z}{Re Z} \quad (2.24)$$

or

$$\text{Re}(Z) = |Z|\cos\phi \quad (2.25)$$

$$\text{Im}(Z) = |Z|\sin\phi \quad (2.26)$$

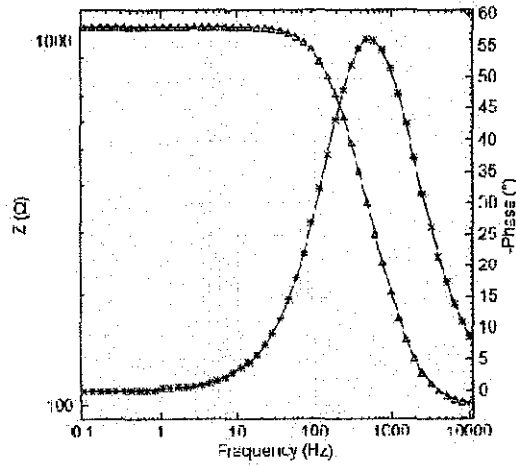


Figure 4: A typical Bode plot

3. METHODOLOGY

3.1 Test Matrix

The test matrix of the experiment and the acetic acid concentration at the said pH value and temperature is shown in Table 1 and Table 2 respectively.

Table 1: Test matrix for the experiment

| Parameter | Value |
|------------------------|---------------------|
| Steel type | X-52 |
| Solution | 3% NaCl |
| De-oxygenation gas | CO ₂ |
| pH | 5.5 |
| Total HAc (ppm) | 0, 1000, 2000, 4000 |
| Temperature (°C) | 60 |
| Time (hrs) | 2 |
| Surface finish | 600 grit |
| Measurement techniques | LPR, EIS, SEM, XRD |

where LPR is linear Polarization Resistance, EIS is electrochemical impedance spectroscopy, SEM is scanning electron microscopy, and XRD is x-ray diffraction. The above test matrix is chosen to reflect conditions in the field.

Table 2: Acetic acid concentration at pH 5.5 and 60°C

| Total Concentration (ppm) | Undissociated HAc (ppm) | Acetate concentration (ppm) |
|---------------------------|-------------------------|-----------------------------|
| 1000 | 154 | 846 |
| 2000 | 308 | 1692 |
| 4000 | 616 | 3384 |

3.2 Experimental Setup

The schematic diagram of the setup is shown in Figure 5.

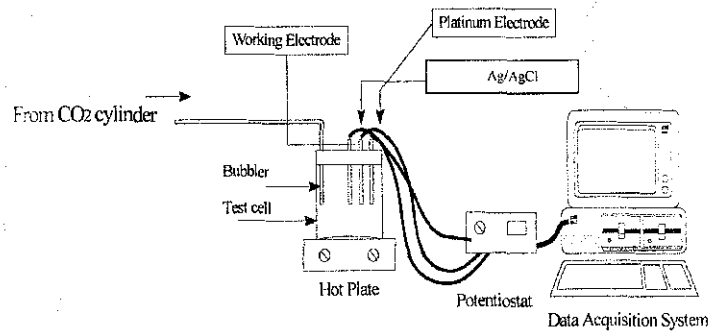


Figure 5: Schematic diagram for the set-up

3.3 Experiment Procedure

The flowchart of the experiment procedure or methodology is shown in Figure 6.

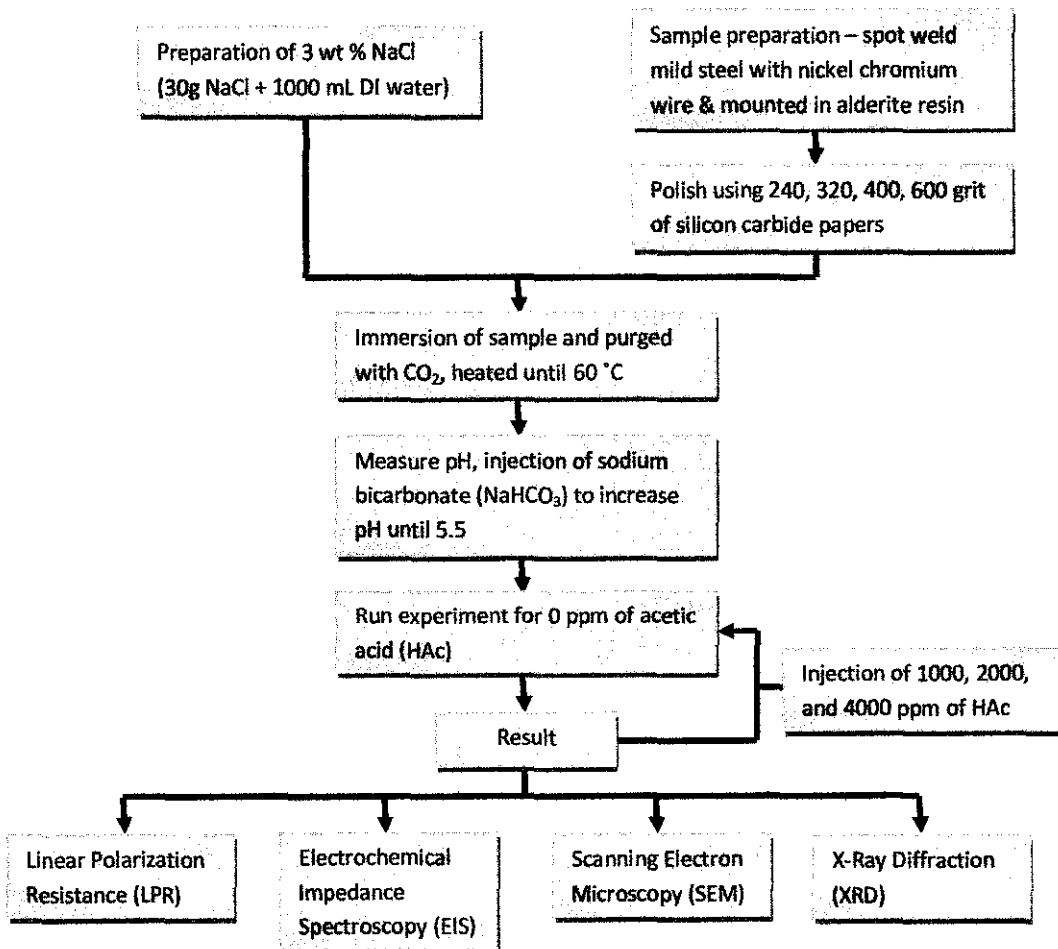


Figure 6: Experiment flowchart

The experiment were performed in a glass cell, on a small scale in order to obtain data quickly and reproducibly. The glass cell was filled with one liter of deionised (DI) water to which 3% by weight of NaCl salt was added. For achieving 3% NaCl concentration, 30g of pure NaCl was weighed and added.

The NaCl solution was then bubbled with CO₂ for 1 hour prior to the exposure of the electrode. CO₂ purging was maintained throughout the test to ensure that all the dissolved oxygen was removed and to maintain the saturation with CO₂. The required test temperature is set through a hot plate. The electrochemical measurements are based on a three-electrode system, using a commercially available potentiostat with a computer control system. The reference electrode used is an Ag/AgCl and the auxiliary electrode is a platinum electrode.

The working electrode is prepared from X52 pipeline steel (elemental composition is shown in Table 3). The sample was spot-welded with nickel-chromium wire and mounted in araldite resin with an exposed area of 0.1 cm². The sample surface is then polished to 600-grade finish using silicon carbide papers. The specimen is degreased and rinsed with ethanol and deionised water before immersion.

The sample is then immersed in the 1 liter of 3% NaCl solution which has been prepared earlier and purged with CO₂ for about 45 minutes while being heated up until the temperature reached the desired value. Then, the pH is measured and 1M of sodium bicarbonate solution is added into the solution until the pH becomes 5.5. The experiment is then ran for 0 ppm of HAC for 2 hours and the data of the LPR and EIS is collected.

The experiment is repeated for different concentrations of HAC injected as stated in the test matrix. The data collected will then be analysed.

Table 3: Elemental composition of X52 carbon steel based on wt %

| Elements | Wt % |
|----------------|---------|
| Carbon (C) | 0.16 |
| Manganese (Mn) | 1.32 |
| Phosphor (P) | 0.017 |
| Sulphur (S) | 0.006 |
| Silicon (Si) | 0.31 |
| Niobium (Nb) | 0.02 |
| Chromium (Cr) | 0.01 |
| Nickel (Ni) | 0.01 |
| Aluminum (Al) | 0.03 |
| Iron (Fe) | Balance |

3.4 Electrochemical Test Methods

Two types of electrochemical studies, linear polarization resistance (LPR) and electrochemical impedance spectroscopy (EIS), were utilized in this study. Linear polarization resistance was used to determine the corrosion rate, while the electrochemical impedance spectroscopy was employed to study the mechanism of CO₂ corrosion in the presence of HAc.

3.4.1 Linear Polarization Resistance (LPR)

This method is based on the linear approximation of the polarization behavior at potentials near the corrosion potential. Polarisation resistance (Rp) is given by Stern-Geary equation:

$$R_p = \frac{B}{i_{corr}} = \frac{\Delta E}{\Delta I} \quad (3.1)$$

$$\text{Where, } B = \frac{b_a b_c}{2.303(b_a + b_c)} \quad (3.2)$$

The value of B used is 26 mV/decade. The corrosion current can be related directly to the corrosion rate from Faraday's law:

$$CR = \frac{315Zi_{corr}}{\rho nF} \quad (3.3)$$

where,

CR = corrosion rate, mm/year

i_{corr} = corrosion current density, $\mu\text{A}/\text{cm}^2$

ρ = density of iron, $7.8 \text{ g}/\text{cm}^3$

F = Faraday's constant, 96500 C/mole

Z = atomic weight, g/mol

n = electron number

b_a, b_c = the slopes of the logarithmic local anodic and cathodic polarization curves respectively

Rp = resistance polarization, ohm

Linear polarization resistance measurements were performed by firstly measuring the corrosion potential of the exposed sample and subsequently sweeping from -10mV to +10mV with the sweep rate of 10mV/min.

3.4.2 Electrochemical Impedance Spectroscopy (EIS)

The EIS set up consists of an electrochemical cell (the system under investigation), a potentiostat, and a frequency response analyser (FRA). The FRA applies the sine wave and analyses the response of the system to determine the impedance of the system.

The electrochemical cell in an impedance experiment can consist of two, three, or four electrodes. The most basic form of the cell has two electrodes. Usually the electrode under investigation is called the working electrode, and the electrode necessary to close the electrical circuit is called the counter electrode. The electrodes are usually immersed in a liquid electrolyte. For solid-state systems, there may be a solid electrolyte or no electrolyte. In this experiment, three electrode systems are used which are the working electrode, the reference electrode, and the auxiliary electrode.

For the potentiostat, experiments were done at a fixed DC potential. A sinusoidal potential perturbation is superimposed on the DC potential and applied to the cell. The resulting current is measured to determine the impedance of the system. The experimental setup for the project is shown in Figure 7.

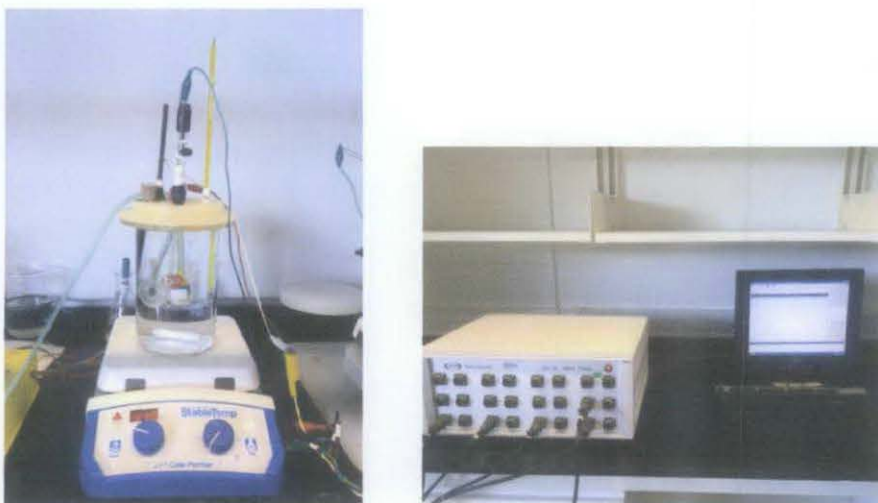


Figure 7: Images of the test set up

3.5 FINAL YEAR PROJECT II GANTT CHART

| NO | ACTIVITIES | WEEK NO/MONTH | | | | | | | | | | | | | | | | | |
|----|---|---------------|--|---|------|---|---|---|------|---|---|---|--------|----|----|-----------|----|----|----|
| | | MAY | | | JUNE | | | | JULY | | | | AUGUST | | | SEPTEMBER | | | |
| | | | | 1 | 2 | 3 | 4 | 5 | 6 | 7 | 8 | 9 | 10 | 11 | 12 | 13 | 14 | 15 | 16 |
| 1 | Experimental Work Continues | | | | | | | | | | | | | | | | | | |
| | 1.1 Sample preparation | | | ■ | ■ | | | | | | | | | | | | | | |
| | 1.2 Run experiment (LPR & EIS) | | | | ■ | ■ | ■ | ■ | ■ | | | | | | | | | | |
| | 1.3 Data gathering and result analysis | | | | | | | | ■ | ■ | | | | | | | | | |
| 2 | Progress Report | | | | | | | | | | | | | | | | | | |
| | 2.1 Submission of progress report | | | | | | | | | | | | | | | | | | |
| | | | | | | | | | | | | | | | | | | | |
| 3 | Experimental Work Continues | | | | | | | | | | | | | | | | | | |
| | 3.1 Run experiment | | | | | | | | | | | | | | | | | | |
| | 3.2 SEM analysis | | | | | | | | | | | | | | | | | | |
| | 3.3 XRD analysis | | | | | | | | | | | | | | | | | | |
| 4 | Pre-EDX | | | | | | | | | | | | | | | | | | |
| | 4.1 Submission of poster | | | | | | | | | | | | | | | | | | |
| | | | | | | | | | | | | | | | | | | | |
| 5 | Dissertation & Oral Presentation | | | | | | | | | | | | | | | | | | |
| | 5.1 Submission of draft report | | | | | | | | | | | | | | | | | | |
| | 5.2 Submission of dissertation (soft bound) | | | | | | | | | | | | | | | | | | |
| | 5.3 Submission of technical paper | | | | | | | | | | | | | | | | | | |
| | 5.4 Oral presentation | | | | | | | | | | | | | | | | | | |
| | 5.5 Submission of project dissertation (hard bound) | | | | | | | | | | | | | | | | | | |

Legend: Δ key milestone

■ progress bar

4.RESULT & DISCUSSION

4.1 Data Gathering & Analysis

The results obtained from the experiment were collected and analyze using the linear polarization resistance (LPR) and electrochemical impedance spectroscopy (EIS) techniques. The sample is then sent for the scanning electron microscopy (SEM) and x-ray diffraction (XRD) analyses. The effects of various concentrations of acetic acid (HAc) from 0 to 4000 ppm on the corrosion behavior of X52 carbon steel in 3% NaCl solution saturated with CO₂ in this experiment are presented below.

4.1.1 Linear Polarization Resistance (LPR) Test

The effect of different concentrations of HAc on the corrosion rates as obtained by LPR test at pH 5.5 and temperature 60°C after 2 hours is shown below.

4.1.1.1 Effect of 0 ppm HAc

The effect of 0 ppm HAc, or in the absence of HAc, on the corrosion rate at pH 5.5 and temperature 60°C after 2 hours is shown in Figure 8.

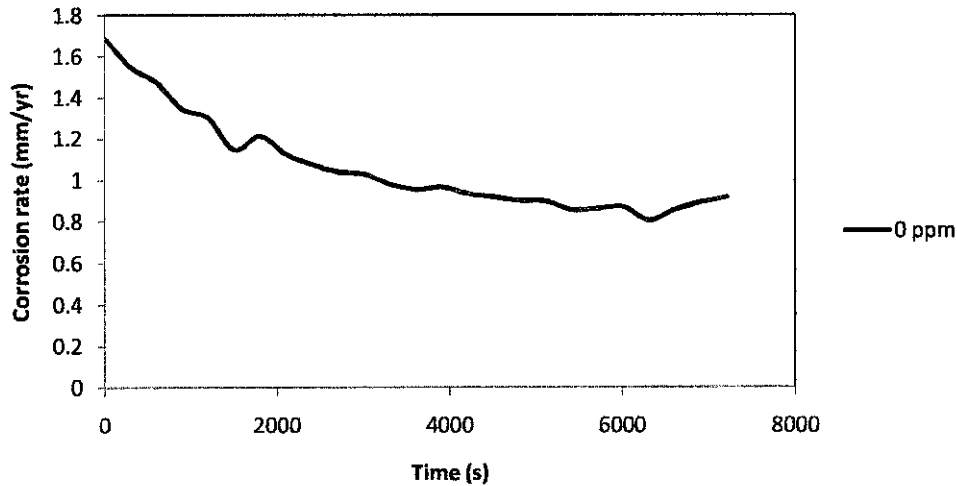


Figure 8: Corrosion rate at 0 ppm of HAc

4.1.1.2 Effect of 1000 ppm HAc

The effect of 1000 ppm HAc, on the corrosion rate at pH 5.5 and temperature 60°C after 2 hours as obtained by the LPR test is shown in Figure 9.

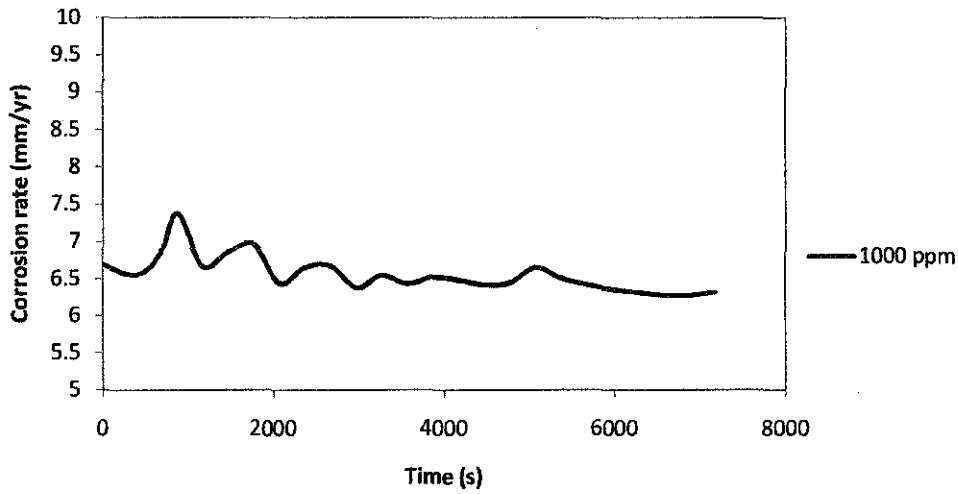


Figure 9: Corrosion rate at 1000 ppm of HAc

4.1.1.3 Effect of 2000 ppm HAc

The effect of 2000 ppm HAc, on the corrosion rate at pH 5.5 and temperature 60°C after 2 hours as obtained by the LPR test is shown in Figure 10.

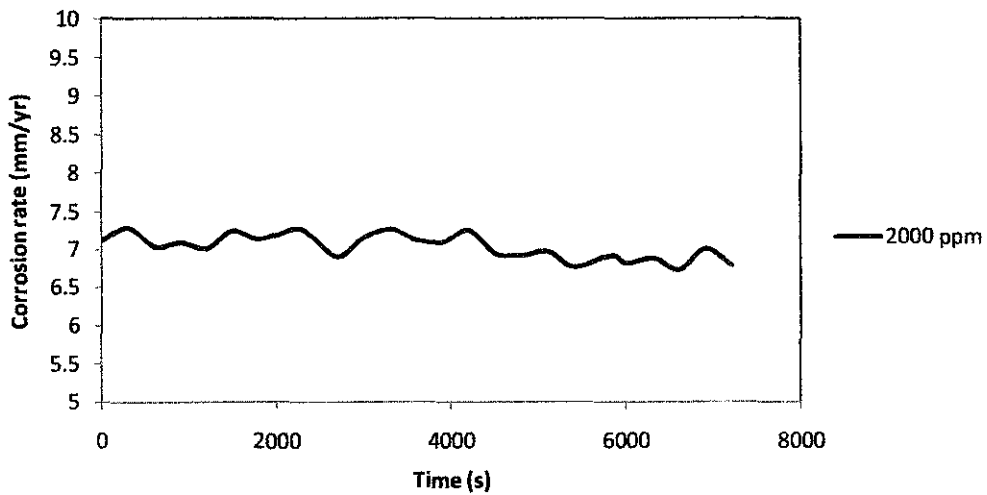


Figure 10: Corrosion rate at 2000 ppm of HAc

4.1.1.4 Effect of 4000 ppm HAc

The effect of 4000 ppm HAc, on the corrosion rate at pH 5.5 and temperature 60°C after 2 hours as obtained by the LPR test is shown in Figure 11.

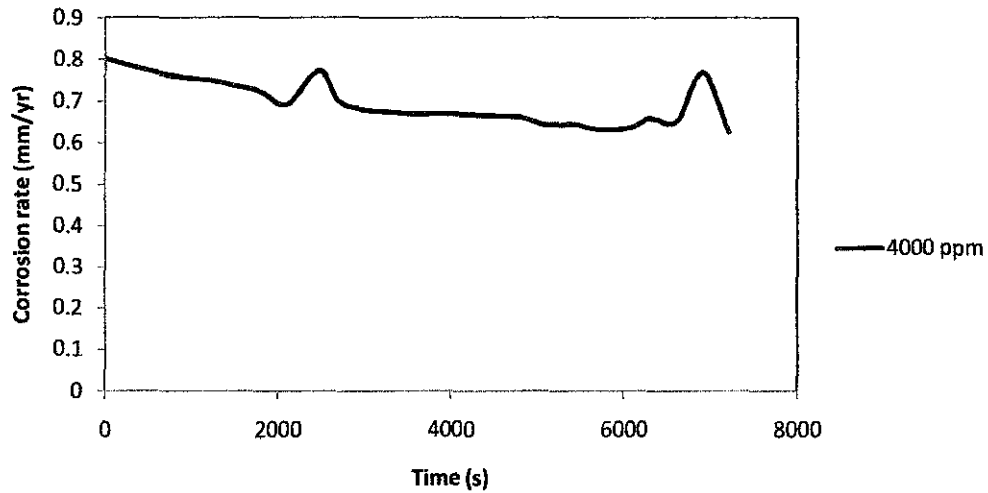


Figure 11: Corrosion Rate at 4000 ppm of HAc

4.1.1.5 Average corrosion rates of different HAc concentrations

The average corrosion rates of X52 carbon steel exposed to concentrations of HAc from 0 to 4000 ppm at pH 5.5 and temperature 60°C are summarized in Figure 12.

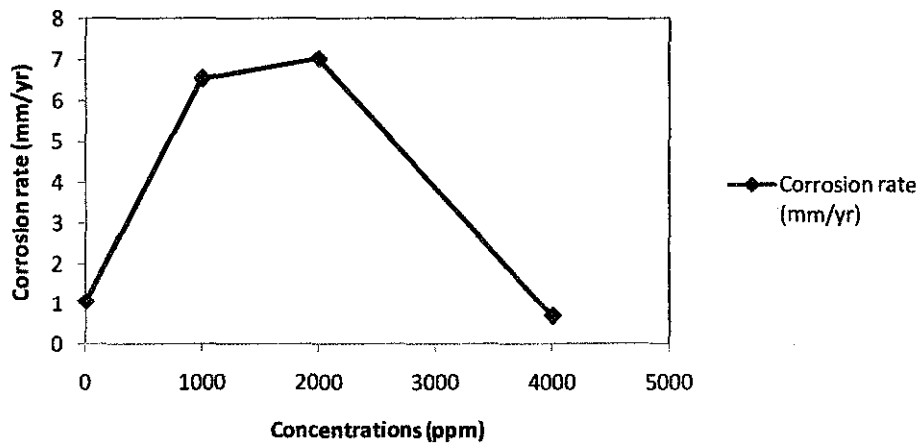


Figure 12: Graph of corrosion rate vs acetic acid concentrations

It is seen that the corrosion rate increase up to approximately 6.5 mm/yr and 7.0 mm/yr with the addition of 1000 ppm and 2000 ppm of acetic acid, respectively. However, the corrosion rate decreased to less than 1 mm/yr with the addition of 4000 ppm of acetic acid.

4.1.1.6 Comparison of the effect of HAc concentrations

The comparison of the effect for different concentrations of HAc, on the corrosion rate at pH 5.5 and temperature 60°C after 2 hours as obtained by the LPR test is shown in Figure 13.

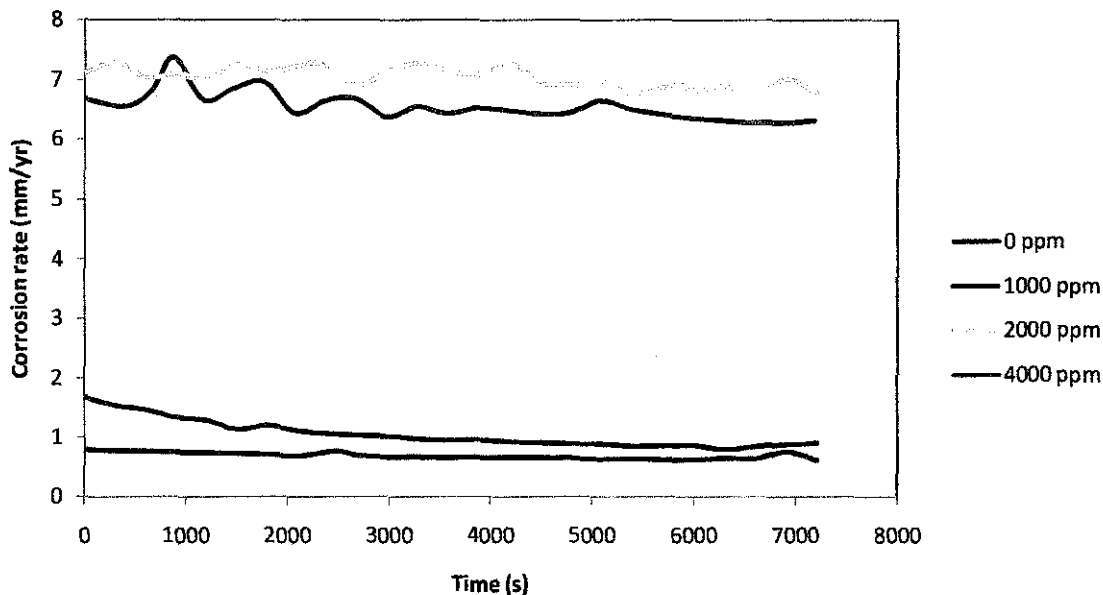


Figure 13: Corrosion Rate at 4 various concentrations of HAc

From Figure 13, it is observed that the corrosion rate in the absence of acetic acid was about 1.7 mm/yr initially and decreased within 2 hours time to values lower than 1 mm/yr as iron carbonate layer formed.

The addition of 1000 ppm and 2000 ppm of acetic acid caused the corrosion rate to increase to approximately 6.5 mm/yr and 7 mm/yr respectively as it interfere with the formation of the film and increases the sensitivity to corrosion attack. This contributes to a lower Fe^{2+} supersaturation in the corrosion film and at the steel surface. The presence of acetate ions (Ac^-) in acetic acid also will tend to solubilize the dissolving iron ions (Fe^{2+}) and suppress iron carbonate layer which can passivate the steel surface. The reaction of Fe^{2+} and Ac^- occurs at a high rate and forms iron(II) acetate ($FeAc$) which is highly soluble in water.

On the other hand, the formation of iron carbonate (FeCO_3) from Fe^{2+} and CO_3^{2-} occurs at a very slow rate as compared to that of FeAc . Therefore, more Fe^{2+} ions will react with Ac^- . The solubility of iron acetate increases as the concentration of acetic acid increases even if the pH is maintained. This results in the increase of the corrosion rate as the exposed area of the steel increase when the solubility of iron acetate increase.

However, the corrosion rate decreased significantly with the addition of 4000 ppm of acetic acid. The corrosion rate dropped to values which was even lower than that of the blank solution (0 ppm). This happens due to the excessive amount of undissociated acetic acid concentration in which the iron carbonate failed to dissolve. In an excessive amount of acetic acid, there might be possibility that FeAc formed much more than its solubility. As a result, FeAc will form another layer of film on the steel surface thus preventing the corrosion from happening.

4.1.2 Electrochemical Impedance Spectroscopy (EIS)

The Nyquist plots obtained for the sample at different concentration of HAc injected at pH 5.5 and temperature 60°C after 2 hours are shown below.

4.1.2.1 Effect of 0 ppm HAc

The Nyquist plot of 0 ppm HAc, or in the absence of HAc, at pH 5.5 and temperature 60°C after 2 hours is shown in Figure 14.

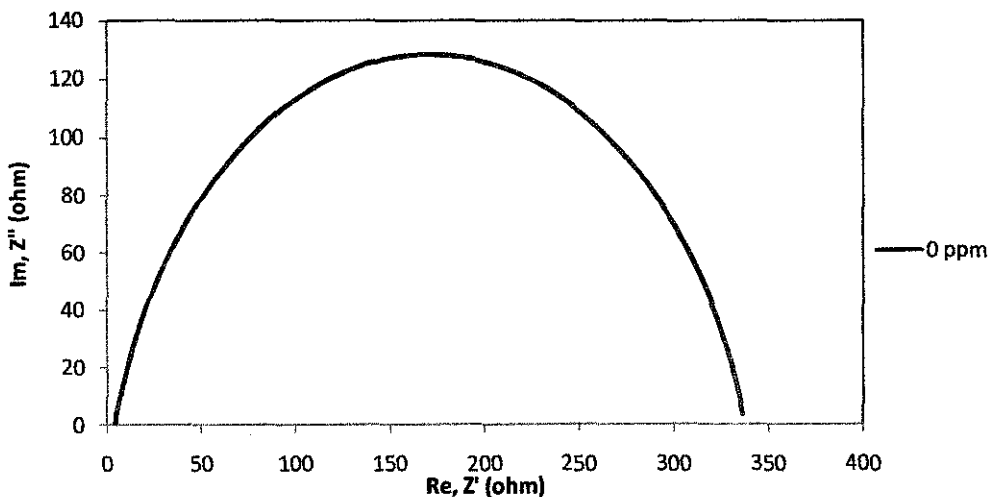


Figure 14: Nyquist plot at 0 ppm of HAc

4.1.2.2 Effect of 1000 ppm HAC

The Nyquist plot of 1000 ppm HAC at pH 5.5 and temperature 60°C after 2 hours obtained by the EIS test is shown in Figure 15.

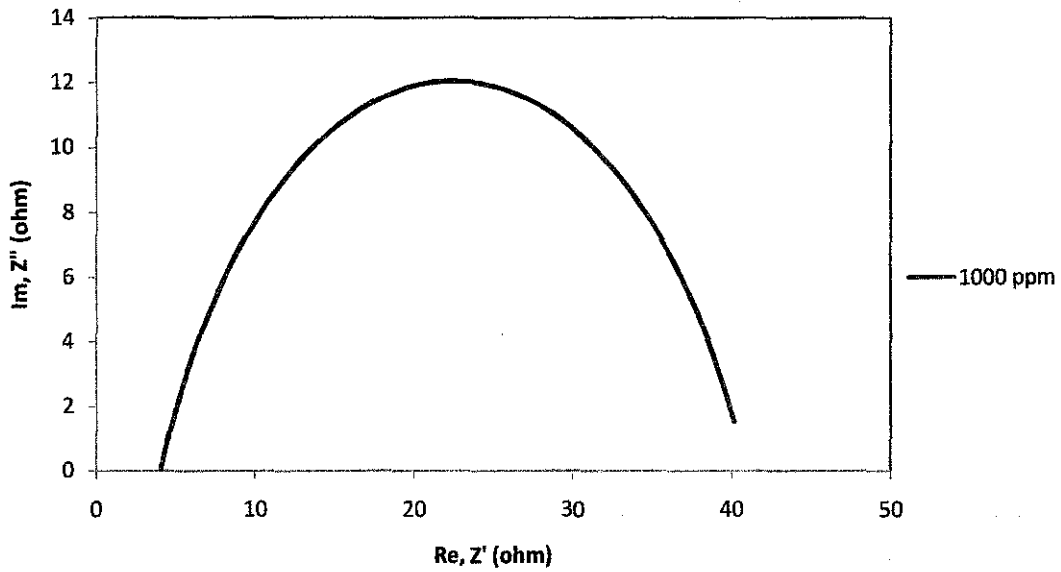


Figure 15: Nyquist plot at 1000 ppm of HAC

4.1.2.3 Effect of 2000 ppm HAC

The Nyquist plot of 2000 ppm HAC at pH 5.5 and temperature 60°C after 2 hours obtained by the EIS test is shown in Figure 16.

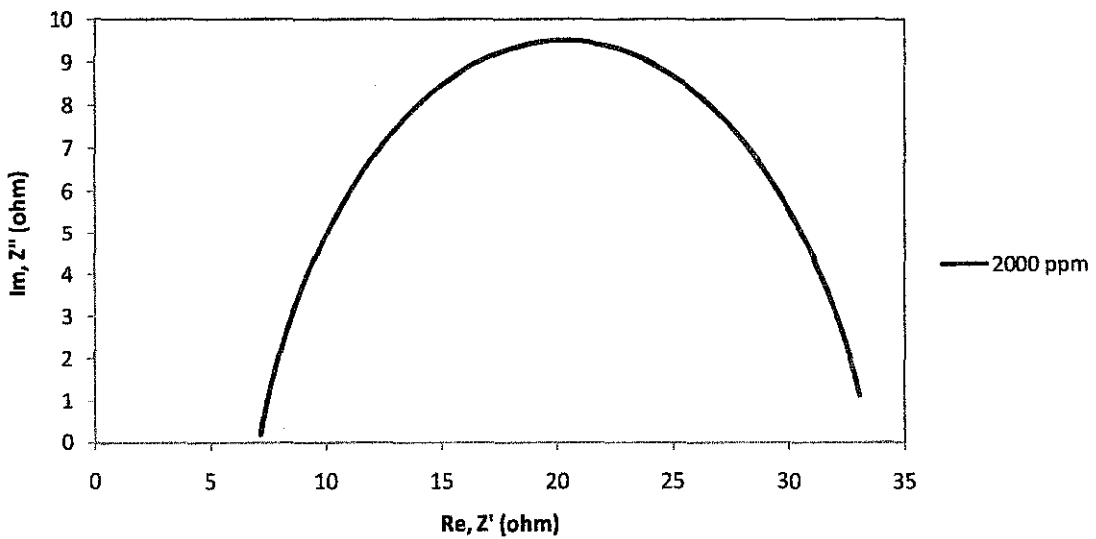


Figure 16: Nyquist plot at 2000 ppm of HAC

4.1.2.4 Effect of 4000 ppm HAc

The Nyquist plot of 4000 ppm HAc at pH 5.5 and temperature 60°C after 2 hours obtained by the EIS test is shown in Figure 17.

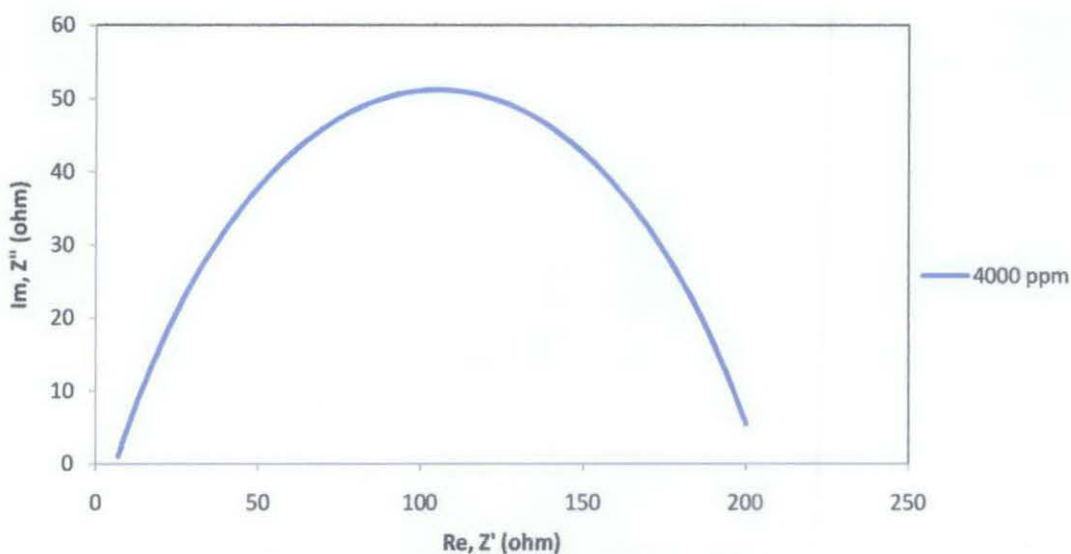


Figure 17: Nyquist plot at 4000 ppm of HAc

4.1.2.5 Comparison of the effect of HAc concentrations

The comparison of the Nyquist plot of 4 different concentrations of HAc at pH 5.5 and temperature 60°C after 2 hours obtained by the EIS test is shown in Figure 18.

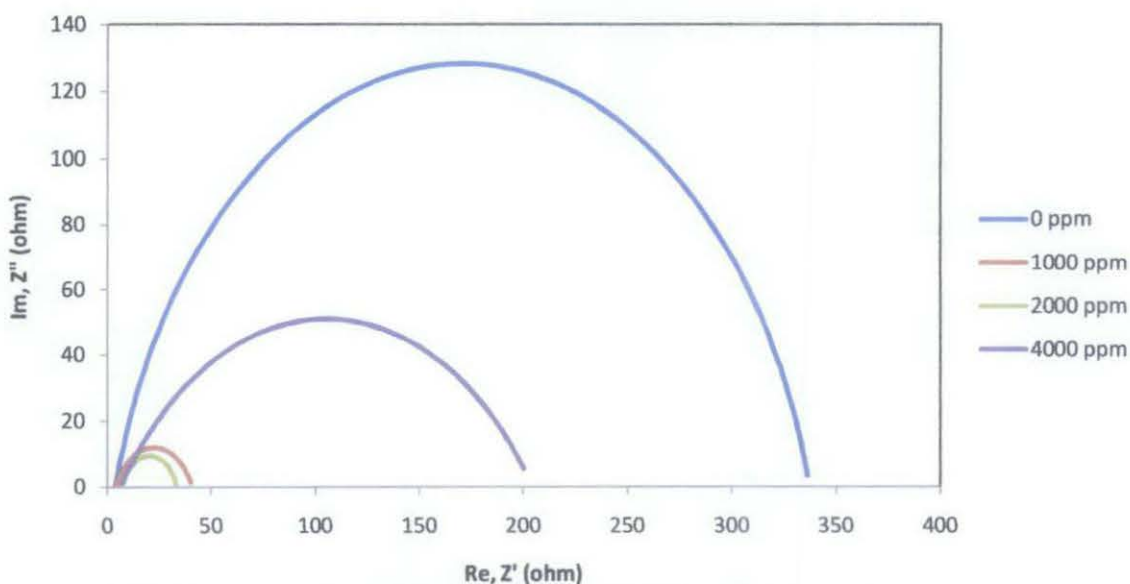


Figure 18: Nyquist plot of the effect of HAc at four different concentrations

Figure 18 shows a very large capacitive loop in the blank solution (0 ppm) and could be considered as the capacitance of double electrode layer between the corrosion scale and solution. This is followed by another capacitive loop for other concentrations of acetic acid.

It is known that iron carbonate film or layer will form and act as a protective scale on the surface of the steel surface if the reaction is given long and enough time to react, preventing the corrosion from happening. When the layer is completely compact, the corrosion is controlled by a diffusion process. However, if there are some pores in the layer, a charge transfer process at the layer/steel interface occurs. This will change the corrosion mechanism to the charge transfer and the shape of impedance plot at low frequencies to a capacitive loop.

According to SEM analysis, a layer of iron carbonate film is formed on the surface of the steel in the absence (0 ppm) of acetic acid. Therefore, it could be deduced that a charge transfer process at the layer/steel interface has occurred in the sample resulting in such a large capacitive loop.

At 1000 ppm of acetic acid, the capacitive loop at diminished significantly and the loop became smaller. It could be seen from the plots that there was a drastic decrease of the impedance values in the presence of 1000 ppm of acetic acid. The shrinkage of the loops shows an increase in corrosion rate and therefore a decrease in the protectiveness of iron carbonate layer. Therefore, active species, such as FeAc, could get to the steel surface easier resulting in an increase of the corrosion rate.

When the concentration of acetic acid is increased to 2000 ppm, the capacitive loop became much smaller than the previous condition as the impedance is diminished. As stated earlier, the shrinkage of the loop means even much less protective iron carbonate layer and an increase in the corrosion rate.

On the other hand, in the presence of 4000 ppm of acetic acid, the capacitive loop expanded and the values of the impedance became bigger. This results from an excessive amount of concentration of undissociated acetic acid injected into the solution. The excessive Ac⁻ ions from the acid reacts with the Fe²⁺ ions from the steel as the rate of reaction of these ions are much higher than that of FeCO₃. This reaction, which forms in a much higher rate than its solubility, will form iron acetate (FeAc) which will act as another protective layer on

the steel surface, thus, reducing the corrosion rate. The presence of the Ac^- ions were confirmed by using XRD techniques which will be discussed later in this chapter.

4.1.3 Scanning Electron Microscopy (SEM) Analysis

The surface condition of the film is then inspected by using the scanning electron microscopy (SEM) technique and the effect of different concentrations of acetic acid (HAc) on iron carbonate film is analyzed with different magnifications. Figure 19 shows the SEM micrographs of the samples with the same magnification of 500X. A very thin layer of iron carbonate was formed on the sample of 0 ppm of HAc. In 1000 ppm of HAc, it seems that the layer of FeAc started to form on the surface due to the effect of the HAc. The formation of the layer is about the same in the presence of 2000 ppm of acetic acid since the rate of solubility of FeAc is high as compared to that of $FeCO_3$. Finally, in the presence of 4000 ppm of HAc, it seems that the formation of FeAc layer increases due to the excessive amount of HAc injected resulting in the decrease of the corrosion rate.

For better insight of this issue we should notice the growth mechanism of iron carbonate layer. The precipitation rate of iron carbonate, R_{FeCO_3} , can be described as below:

$$R_{FeCO_3} = Af(T)K_{sp}f(S) \quad (4.1)$$

where A refers to the surface area of the sample, T is the temperature, K_{sp} is denotes the solubility limit of iron carbonate and S is the supersaturation. Regarding the conditions under present investigation, the only variable parameter in equation (4.1) is supersaturation level. The sample in the absence of HAc had the most supersaturation since there was no interference by the HAc, so it has the most precipitation rate leading to the most dense iron carbonate film followed by the sample with 1000, 2000, and 4000 ppm of HAc respectively.

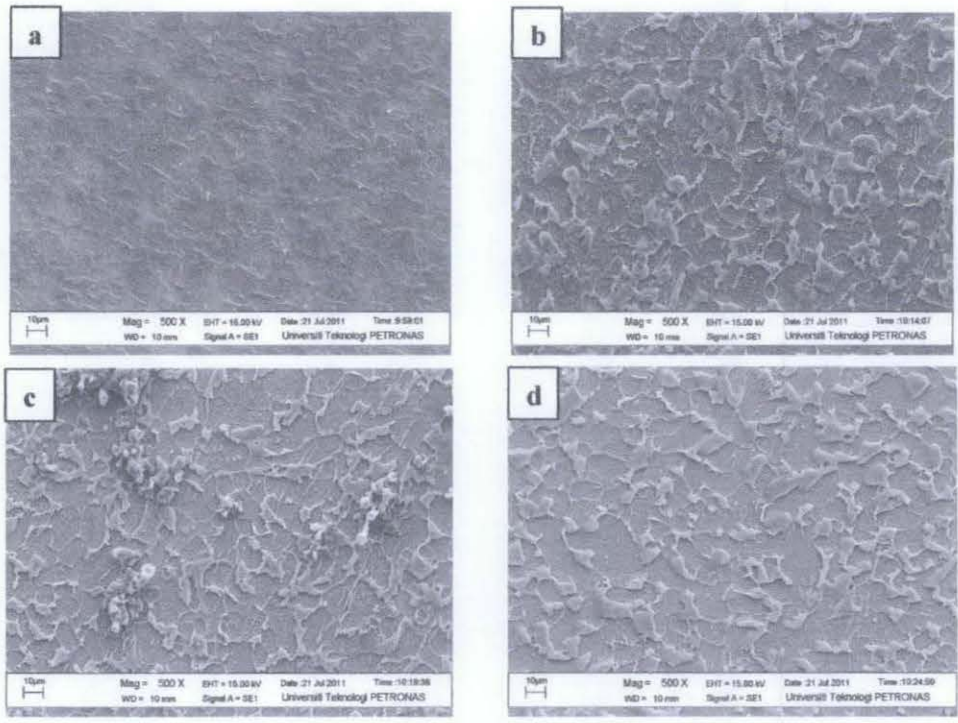
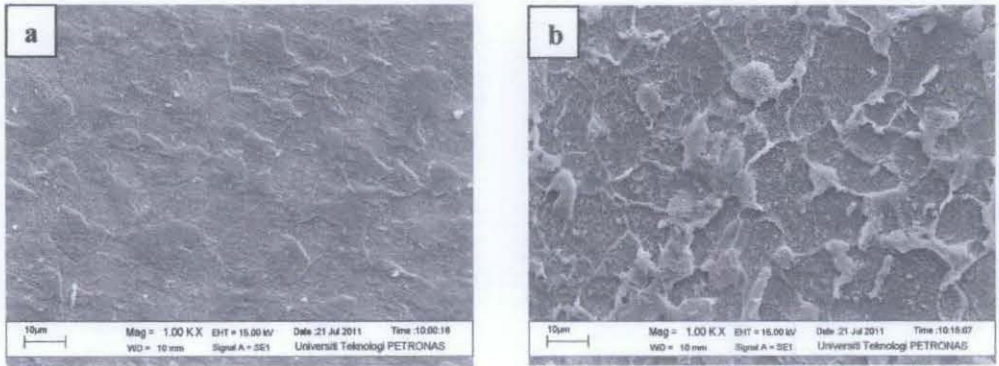


Figure 19: SEM micrographs for X52 carbon steel achieved after 2 h of exposure in CO₂-saturated 3wt% NaCl solution at the temperature of 60°C under 500X magnification in the presence of (a) 0, (b) 1000, (c) 2000, and (d) 4000 ppm of acetic acid

Figure 20 shows the SEM micrographs of the samples with different concentrations of HAC viewed under the same magnification of 1000X.



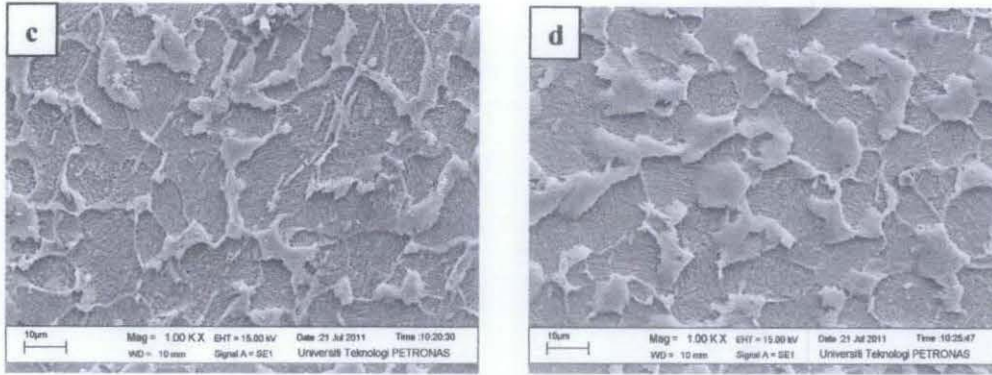


Figure 20: SEM micrographs for X52 carbon steel achieved after 2 h of exposure in CO₂-saturated 3wt% NaCl solution at the temperature of 60°C under 1000X magnification in the presence of (a) 0, (b) 1000, (c) 2000, and (d) 4000 ppm of acetic acid

Figure 21 shows the SEM micrographs of the samples with different concentrations of HAC viewed under the same magnification of 5000X.

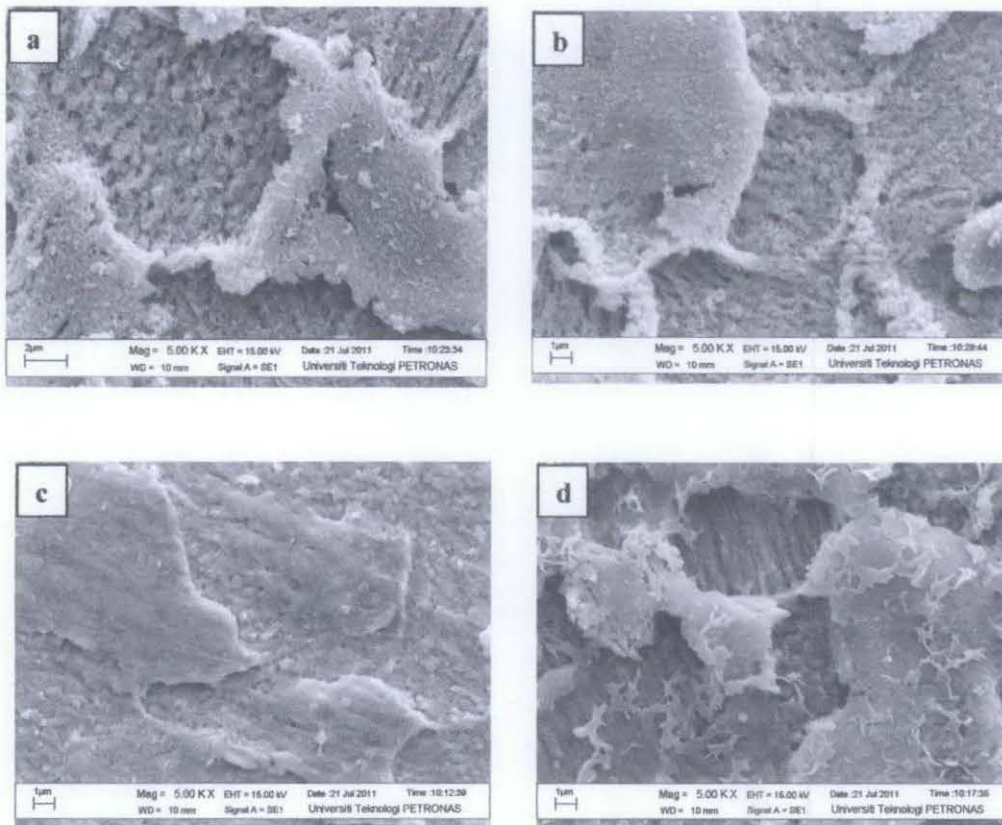


Figure 21: SEM micrographs for X52 carbon steel achieved after 2 h of exposure in CO₂-saturated 3wt% NaCl solution at the temperature of 60°C under 5000X magnification in the presence of (a) 0, (b) 1000, (c) 2000, and (d) 4000 ppm of acetic acid

4.1.4 X-Ray Diffraction (XRD) Analysis

X-Ray Diffraction (XRD) was used in order to evaluate if there are any other compounds other than iron carbonate (FeCO_3) which could be identified on the steel surface. XRD result in Figure 22 shows the comparison of analysis of the sample without the presence of the acetic acid and with 4000 ppm of acetic acid. It is seen that the main iron peak on the sample without the acetic acid (black) is higher than that with 4000 ppm of acetic acid (red) which means all of the iron ions (Fe^{2+}) is present prior to react with the carbonate (CO_3^{2-}). The main iron peak with 4000 ppm of acetic acid became lower since some of the Fe^{2+} ions has reacted with the Ac^- ions to form iron acetate (FeAc).

Figure 23 shows the XRD analysis on the sample in the absence of acetic acid. It shows the presence of only iron (blue) and iron carbonate (red), without any interference from any other compound.

On the other hand, in the presence of 4000 ppm of acetic acid, the XRD signal in Figure 24 shows the presence of another compound which is iron acetate (green peak) as discussed in the EIS part earlier. The concentration of acetic acid seems to have exceeded the solubility limit of iron carbonate film, thus, allowing the reaction of iron ions and acetate ions to take place to form iron acetate. This reaction forms another protective layer resulting in the decrease of the corrosion rate.

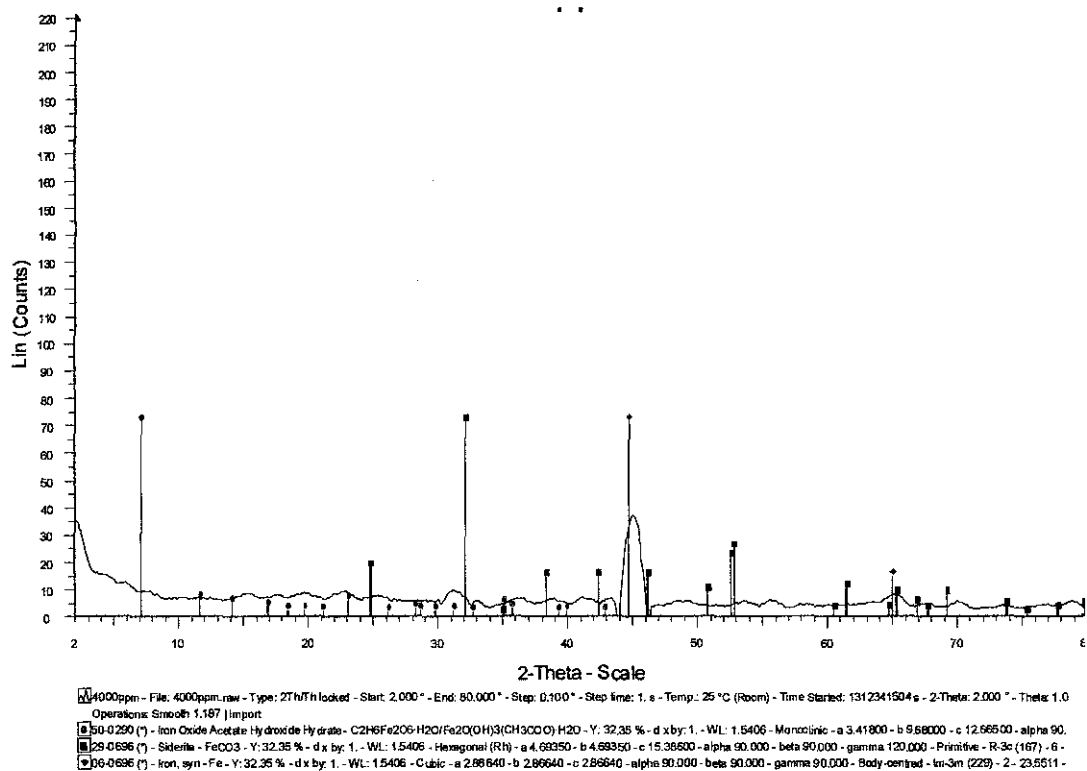


Figure 24: XRD analysis of the layer formed on the X52 carbon steel at pH 5.5 and T=60°C in the presence of 4000 ppm of undissociated acetic acid after 2h.

5. CONCLUSION & RECOMMENDATIONS

Based on the results obtained, the corrosion rate increased with the addition of 1000 ppm and 2000 ppm of acetic acid. However, with the addition of 4000 ppm of acetic acid, the corrosion rate decreased.

In the absence of acetic acid, a very thin layer of iron carbonate was formed on the steel surface as a chief corrosion product of the mechanism. The corrosion product is produced from the reaction of the iron ions and the carbonate ions. In the presence of 1000 ppm of acetic acid, the corrosion rate started to increase as the acetate ions from the acid tends to solubilize the dissolving iron ions and suppress iron carbonate layer which can passivate the steel surface. The solubility of iron acetate increases as the concentration of acetic acid increases. Thus, the presence of 2000 ppm of acetic acid will expose the surface of the steel even more and increase the corrosion rate.

On the other hand, in the presence of 4000 ppm of acetic acid, the corrosion rate decreased significantly and is believed due to the excessive amount of concentration of acetate ions in the solution. The carbonate ions from the iron carbonate could not dissolve the excessive amount of acetate leaving the iron ions to reacts with it and form iron acetate. The presence of the iron acetate is shown in the XRD result. This new compound will form another layer on the steel surface thus reducing the corrosion rate. However, it is still not clear how the iron acetate compound will affect the steel surface.

It is recommended that the period of the experiment is added in order to obtain more accurate results and much clearer picture in the SEM micrograph. The energy dispersive x-ray (EDX) analysis also should be done in order to confirm the presence of any compound on the steel surface.

REFERENCES

1. Omkar A. Nafday, August 2004, "Film Formation CO₂ Corrosion in the Presence of Acetic Acid" in Fritz J. And Dolores H. Russ College of Engineering and Technology of Ohio University
2. M.C. Ismail, 2006, "Prediction Equation of CO₂ Corrosion With the Presence of Acetic Acid", Universiti Teknologi PETRONAS, and S.Turgoose, C&APC, UMIST
3. Martin Choirul Fatah, April 2009, "Prediction of CO₂ Corrosion with the Presence of Low Concentrations Acetic Acid in Turbulent Flow Conditions", Universiti Teknologi Petronas
4. Egil Gulbrandsen, 2007, "Acetic Acid and Carbon Dioxide Corrosion of Carbon Steel Covered with Iron Carbonate", Institute of Energy Technology, Instituttveien 18
5. M.B Kermani and A. Morshed, August 2003, "Carbon Dioxide Corrosion in Oil and Gas Production – A Compendium", University College London, Torrington Place, United Kingdom.
6. Mehdi Honarvar Nazari, Saeed Reza Allahkaram, April 2010, "The Effect of Acetic Acid on the CO₂ Corrosion of Grade X70 Steel", University College of Engineering, University of Tehran, North Kargar, Tehran
7. Vanessa Fajardo, Christian Canto, Bruce Brown, David Young and Srdjan Netic, 2008, "The Effect of Acetic Acid on the Integrity of Protective Iron Carbonate Layers in CO₂ Corrosion of Mild Steel", Ohio University, Institute for Corrosion and Multiphase Technology, Athens.
8. G.A. Zhang, Y.F. Cheng, April 2009, "Corrosion of X65 Steel in CO₂-saturated Oilfield Formation Water in the Absence and Presence of Acetic Acid", University of Calgary, Calgary, Alberta, Canada.
9. Vanessa Fajardo, Christian Canto, Bruce Brown, David Young and Srdjan Netic, 2007, "Effect of Organic Acids in CO₂ Corrosion", Ohio University, Institute for Corrosion and Multiphase Technology, Athens.
10. J. Amri, E. Gulbrandsen, R.P. Nogueira, "The Effect of Acetic Acid on the Pit Propagation in CO₂ Corrosion of Carbon Steel", Institute of Energy Technology, Norway.
11. Omkar A. Nafday and Srdjan Netic, "Iron Carbonate Scale Formation and CO₂ Corrosion in the Presence Of Acetic Acid", Institute for Corrosion and Multiphase Technology, Ohio University, Athens.
12. J.L. Crolet, N. Thevenot, and A. Dugstad, "Role of Acetic Acid on the CO₂ Corrosion of Steel", CORROSION/99, Paper No. 24 (Nace International, 1999, Houston, Texas).

13. M.W. Joosten, J. Kolts, J.W. Hembree, and M. Achour, "Organic Acid Corrosion in Oil and Gas Production", CORROSION/2002, Paper No. 02294 (Nace International, 2002, Houston, Texas).
14. K.S. George, March, 2003, "Electrochemical Investigation of Carbon Dioxide Corrosion of Mild Steel in the Presence of Acetic Acid", Fritz J. And Dolores H. Russ College of Engineering and Technology of Ohio University.
15. Y.Garsany and D.Pletcher, "The Role of Acetate in CO₂ Corrosion of Carbon Steel: Has The Chemistry Been Forgotten?", CORROSION/2002, Paper No. 02273 (Nace International, 2002, Houston, Texas).
16. X.P. Guo, Z.Y. Chen, D. Liu, K. Bando, and Y.Tomoe, "The Effect of Acetic Acid and Acetate on CO₂ Corrosion of Carbon Steel",CORROSION/2005, Paper No. 05306 (Nace International, 2005, Houston, Texas).